

Zn-impurity effect and interplay of s_{\pm} - and s_{++} -pairings in Fe-based superconductors

Zi-Jian Yao¹, Wei-Qiang Chen^{2,1}, Yu-ke Li³, Guang-han Cao⁴,
Hong-Min Jiang^{1,3}, Qian-En Wang¹, Zhu-an Xu⁴, Fu-Chun Zhang^{1,4}
¹ *Department of Physics and Center of Theoretical and Computational Physics,
The University of Hong Kong, Hong Kong, China*
² *Department of Physics,
South University of Science and Technology of China, Shenzhen, China*
³ *Department of Physics,
Hangzhou Normal University, Hangzhou, China*
⁴ *Department of Physics,
Zhejiang University, Hangzhou, China*

(Dated: November 23, 2018)

We report theoretical and experimental studies of the effect of Zn-impurity in Fe-based superconductors. Zn-impurity is expected to severely suppress sign reversed s_{\pm} wave pairing. The experimentally observed suppression of T_c under Zn-doping strongly depends on the materials and the charge carrier contents, which suggests competition of s_{++} and s_{\pm} pairings in Fe-base superconductors. We study a model incorporating both s_{++} and s_{\pm} pairing couplings by using Bogoliubov de-Gennes equation, and show that the Zn-impurity strongly suppresses s_{\pm} pairing and may induce a transition from s_{\pm} to s_{++} -wave. Our theory is consistent with various experiments on the impurity effect. We present new experimental data on the Zn-doping $\text{SmFe}_{1-x}\text{Zn}_x\text{AsO}_{0.9}\text{F}_{0.1}$ of $T_c = 50\text{K}$, in further support of our proposal.

PACS numbers:

I. INTRODUCTION

One of the most important issues in the high T_c Fe-based superconductors (FeSC) is their pairing symmetry [1–3]. Theories based on antiferromagnetic (AF) spin fluctuations have predicted s_{\pm} pairing, where the superconducting (SC) order parameters on the hole and electron Fermi pockets have opposite signs [4, 5]. The proposed symmetry is consistent with a number of experiments, such as the spin resonance peak in neutron scattering [6], sensitive SC junction data [7, 8], and quasi-particle interference in tunneling experiments [9]. However, the pairing symmetry in FeSC may not be universal, and there are evidences for different pairing structures as discussed in a recent review [10].

The effect of disorder to the superconductivity is an important test to the pairing symmetry. According to Anderson's theorem, the conventional s-wave superconductivity is insensitive to non-magnetic impurities. The sign reversed s_{\pm} superconductivity is, however, sensitive to non-magnetic impurities which scatter inter-band electrons. Replacement of part of Fe-atoms by Co or Ni in a parent compound of FeSC leads to superconductivity. However, the role of the Co or Ni doping is more subtle and remains controversial. One scenario is that the doping introduces additional electron carriers. This scenario is supported by the angle resolved photoemission spectroscopy, which indicates the shrinking of the hole pockets [11]. On the other hand, recent resonant photoemission spectroscopy and density functional calculations indicate that Co doping is covalent and introduces disorder [12]. It is plausible that the Co doping introduces both carriers and disorder [13]. Zn-ion has

a $3d^{10}$ configuration, hence a very high electric potential to charge carriers. Replacing a Fe-atom by Zn in FeSC introduces inter-band scattering and is expected to severely suppress the s_{\pm} superconductivity. Therefore, the Zn-doping is an effective test to the s_{\pm} pairing in FeSC. There have been several experiments on the Zn-doping effect on FeSC, including so-called 1111 compounds $\text{LaFe}_{1-x}\text{Zn}_x\text{AsO}_{1-y}\text{F}_y$ [14, 15], and more recently 122 compounds $\text{BaFe}_{2(1-x-y)}\text{Zn}_{2x}\text{Co}_{2y}\text{As}_2$ and $\text{SrFe}_{1.8-2x}\text{Zn}_{2x}\text{Co}_{0.2}\text{As}_2$ [16]. The results are mixed at present, which appears to be strongly dependent of material and charge carrier content. The experimental data on the 1111 compounds may be divided into two categories. The optimally doped $\text{LaFeAsO}_{0.9}\text{F}_{0.1}$ [14] is insensitive, but the over-doped $\text{LaFeAsO}_{0.85}\text{F}_{0.15}$ is very sensitive to the Zn-impurities [15]. The effect of Zn-doping on Co-doped 122 compounds clearly shows the suppression of superconducting transition temperature T_c , but the reduction is much slower than the theory predicted [16]. A careful examination indicates that the suppression of T_c may be saturating at large Zn-doping to some of the compounds. Note that it is not easy to dope Zn into the Fe lattices uniformly even under high pressure, and reliable data is only available up to 6% Zn-doping at present. Therefore the experimental data are not complete. Nevertheless, the available experiments on Zn-doping indicate complexity of the effect, and suggest possible competition of sign changed s_{\pm} and sign unchanged s_{++} pairings in FeSC.

In this paper, we use a two-orbital model for FeSC including both on-site (or s_{++}) pairing coupling g_0 and next nearest neighbor (NNN) intersite (or s_{\pm}) pairing coupling g_2 to study Zn-impurity effect, which may help

understand the complex result of the Zn doping effect on 1111 and 122 compounds. We apply Bogliubov de-Gennes (BdG) equation to study the model on a finite-size system. The two SC pairings in the multi-band system show interesting interplay. They may mix but also compete with each other. The disorder strongly suppresses the intersite pairing, and its effect to the superconductivity depends on the strength of g_0 . For large g_0 , g_2 plays little role and the pairing is s_{++} and is robust against the disorder. For small g_0 , the pairing is s_{\pm} and the disorder strongly suppresses superconductivity. For moderate value of g_0 , the disorder may enhance the on-site pairing and induce a transition from s_{\pm} to s_{++} superconductivity. We further study the interplay between g_0 and g_2 in a clean system and show that the disorder effect on the gap functions is similar to the reduction of g_2 . Our theory is consistent with the Zn-doped impurity experiments on 1111 and 122 compounds, and suggests multi-pairing couplings in some of the FeSC. We present our new experimental data of the Zn-impurity effect on the very high $T_c = 50\text{K}$ Sm-1111 compound. The lattice constant measurement show that the Zn-atoms are doped into the Fe-lattice uniformly up to 6%. The results appear to indicate possible saturation of T_c under the Zn doping, consistent with the present theory.

II. MODEL HAMILTONIAN AND MEAN FIELD THEORY

We consider a model Hamiltonian

$$H = H_0 + H_{\text{pair}} + H_{\text{imp}}, \quad (1)$$

which includes a tight-binding kinetic term H_0 , a pairing interaction H_{pair} , and a disordered term H_{imp} . For H_0 , we consider a two-orbital model with d_{xz} (orbital 1) and d_{yz} (orbital 2) as proposed by Raghu et al. [17].

$$H_0 = \sum_{(i\alpha, j\beta)\sigma} C_{i\sigma}^\dagger \hat{h}_{ij} C_{j\sigma}, \quad (2)$$

where $C_{i\sigma}^\dagger = (c_{i1,\sigma}^\dagger, c_{i2,\sigma}^\dagger)$, and $\hat{h}_{ij}^{\alpha,\beta} = t_{i,j}^{\alpha,\beta}$ is the electron hopping term between orbital α at site i and orbital β at site j on a 2-dim. square lattice of Fe-atoms (lattice constant $a = 1$). While this model may be an oversimplified one to describe many detailed material properties of FeSC, it should capture the basic feature of the disorder effect to the pairing in systems with multi-Fermi surfaces. The non-vanishing hopping matrix elements are $t_{i,i}^{\alpha\alpha} = -\mu$, $t_{i,i+\hat{y}}^{11} = t_2$, $t_{i,i+\hat{y}}^{22} = t_1$, $t_{i,i+\hat{x}+\hat{y}}^{\alpha\alpha} = t_3$, $t_{i,i+\hat{x}+\hat{y}}^{12} = t_{i,i+\hat{x}+\hat{y}}^{21} = -t_4$. We choose $t_1 = 1$ as the energy unit, and $\mu = 1.6$, $t_2 = -1.3$, $t_3 = t_4 = 0.85$, which gives Fermi surfaces with hole pockets near the Γ - and M points, and electron pockets near the X - and Y points in an extended Brillouin zone as plotted in Fig. 1.

We consider randomly distributed impurities on the lattice and introduce an on-site repulsive potential on

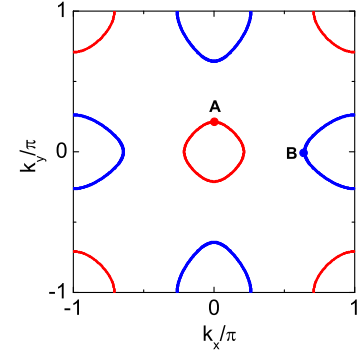


FIG. 1: (Color online) Hole (red) and electron (blue) Fermi pockets obtained in the two-orbital model Eq. (2). Points A and B are the representative \vec{k} points for the hole and electron pockets, respectively.

the Zn-impurity site,

$$H_{\text{imp}} = I \sum_{i \in \text{imp}} \sum_{\sigma} C_{i\sigma}^\dagger C_{i\sigma}, \quad (3)$$

where i sums over all the impurity sites, and we consider the large I case ($I = 24t_1$ in the actual calculation) to model the large repulsion to an electron at the Zn site. The pairing Hamiltonian is modeled by

$$H_{\text{pair}} = - \sum_{\langle ij \rangle} (V_{ij} c_{i\alpha\uparrow}^\dagger c_{j\beta\downarrow}^\dagger c_{j\beta\downarrow} c_{i\alpha\uparrow} + h.c.), \quad (4)$$

where the pairing coupling V_{ij} includes an on-site term $g_0 > 0$ and an NNN intersite term g_2 ,

$$V_{ij} = g_0 \delta_{i,j} + g_2 \sum_{\vec{\tau}} \delta_{j,i+\vec{\tau}}. \quad (5)$$

with $\vec{\tau}$ the vector of the two NNN site displacement. Note that g_0 term favors s_{++} and g_2 term favors s_{\pm} symmetry.

We introduce a mean field gap function $\Delta_{ij}^{\alpha\alpha} = V_{ij} \langle c_{j\alpha\downarrow} c_{i\alpha\uparrow} \rangle$. Our calculations show that the inter-orbital pairing Δ_{ij}^{12} is very tiny and will be neglected below. The BdG equation for the mean field Hamiltonian then reads

$$\sum_j \begin{pmatrix} \hat{h}_{ij} & \hat{\Delta}_{ij} \\ \hat{\Delta}_{ij}^* & -\hat{h}_{ij,\bar{\sigma}}^* \end{pmatrix} \begin{pmatrix} \mathbf{u}_{j,\sigma}^n \\ \mathbf{v}_{j,\bar{\sigma}}^n \end{pmatrix} = E_n \begin{pmatrix} \mathbf{u}_{i,\sigma}^n \\ \mathbf{v}_{i,\bar{\sigma}}^n \end{pmatrix}, \quad (6)$$

with $\hat{\Delta}_{ij} = \Delta_{ij} \hat{I}$, and \hat{I} an identity matrix. $\mathbf{u}_{i,\sigma} = \begin{pmatrix} u_{i1,\sigma} \\ u_{i2,\sigma} \end{pmatrix}$. The self-consistent equation for the gap function is

$$\Delta_{ij}^{\alpha\alpha} = \frac{V_{ij}}{4} \sum_n (u_{i\alpha,\sigma}^n v_{j\alpha,\bar{\sigma}}^{n*} + v_{i\alpha,\bar{\sigma}}^{n*} u_{j\alpha,\sigma}^n) \times \tanh\left(\frac{E_n}{2k_B T}\right) \quad (7)$$

For the form of V_{ij} in Eq. (5), we define $\Delta_0^{\alpha\alpha}(i) = \Delta_{ii}^{\alpha\alpha}$, and $\Delta_2^{\alpha\alpha}(i) = \sum_{\vec{\tau}} \Delta_{i,i+\vec{\tau}}^{\alpha\alpha}/4$.

III. NUMERICAL RESULTS

We now discuss the numerical solutions of H . In our calculations, for each impurity content, the impurity positions are randomly distributed and the statistical averages are taken over 400 times. We consider three typical cases: (i) g_0 is large and dominant; (ii) g_2 is large and g_0 is weak; and (iii) g_2 is dominant but g_0 is moderately large. In case (i), the SC pairing is always s_{++} and the superconductivity is robust against the impurity as we expect from the Anderson theorem.

In Fig. 2 (a) and (b), we show the spatially averaged on-site and NNN inter-site pairing amplitudes $\Delta_0 = \Delta_0^{\alpha\alpha}$ and $\Delta_2 = \Delta_2^{\alpha\alpha}$ as functions of the impurity concentration n_{imp} for cases (iii) and (ii). Also shown are the gaps at the hole pocket (point A $[(0, 0.22\pi)]$) and at the electron pocket (point B $[(0.62\pi, 0)]$), which are the Fourier transform of the impurity averaged gaps in real space. In the case (ii) of weak on-site pairing, the impurities strongly suppress Δ_2 as shown in the Fig. 2(b). Δ_0 is tiny and the SC gap functions Δ_A and Δ_B monotonically decrease as n_{imp} increases. Because of the finite lattice size, our study is limited to the short coherence length or the strong pairing coupling cases, which require $n_{\text{imp}} \approx 0.15$ to destroy the superconductivity. We expect this value to be much smaller in weaker pairing coupling cases.

Case (iii) is most interesting, and our theory shows an impurity driven phase transition from s_{\pm} to s_{++} pairings. In the absence of impurity, g_2 dominates and the pairing is s_{\pm} . As shown in Fig. 2(a), the pairing symmetry remains to be s_{\pm} at $n_{\text{imp}} < 0.02$, and the gap amplitudes on k points A and B are monotonically suppressed as n_{imp} increases. At $0.02 < n_{\text{imp}} < 0.05$, $|\Delta_2|$ decreases, and $|\Delta_0|$ increases. At $n_{\text{imp}} > 0.05$, both Δ_A and Δ_B are positive and we have s_{++} pairing. It is interesting to note that the on-site pairing may be enhanced by the impurities due to the suppression of the NNN pairing.

In the case of weak on-site pairing, as shown in Fig. 2(b), the impurities strongly suppresses Δ_2 . We have examined the SC order parameters in real space and found that the disorder does not result in severe pair-breaking effect to the on-site pairing measured by $\Delta_{i,i}^{\alpha\alpha}$, whose peak amplitude is almost unaltered by the impurities. On the other hand, the non-magnetic impurities not only destroy NNN SC pairing order parameter $\Delta_{i,i+\hat{x}+\hat{y}}^{\alpha\alpha}$ in larger spatial areas, but also weaken the peak amplitude of the SC pairing immensely.

As we have demonstrated, the impurities suppress the NNN pairing order parameter Δ_2 . This effect is similar to the reduction of g_2 in the clean sample. Therefore, tuning n_{imp} in the disorder system is similar to tuning g_2 in a clean system [18]. Below we shall study SC order parameters and T_c in the model Hamiltonian H as functions of g_2 in the absence of disorder to mimic the impurity effect. This enables us to further reveal the interplay between the SC pairings of s_{++} and s_{\pm} .

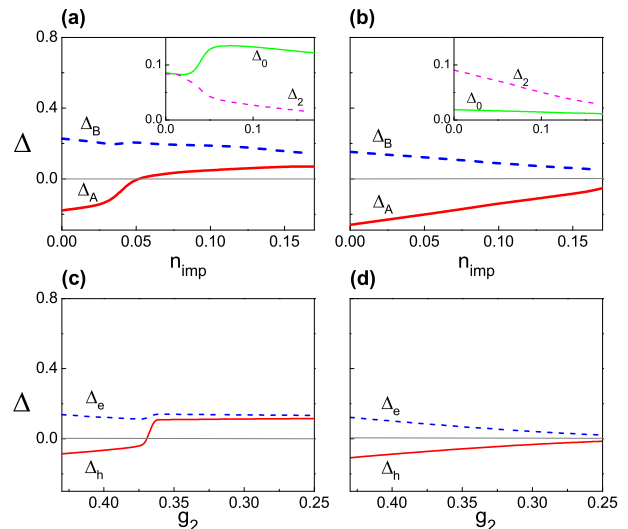


FIG. 2: (Color online) Upper panel: The gap functions at hole and electron Fermi pockets Δ_h and Δ_e as functions of impurity density n_{imp} , obtained in the mean field solution for H . (a): for modestly strong on-site pairing coupling $g_0 = 1.8$; (b): for weak on-site coupling $g_0 = 0.8$. Insets: spatially averaged gap functions Δ_0 (on-site) and Δ_2 (NNN inter site). In both cases, the NNN coupling $g_2 = 1.6$. Lower panel: SC gaps calculated by the simplified BCS formalism, with $N_e(0) = 0.12$, $N_h(0) = 0.1$, and $\omega_D = 0.8$. (c): $g_0 = 1.8$; (d): $g_0 = 0.8$.

IV. T_c REDUCTION: THEORY AND EXPERIMENTS

For a clean system, we have lattice translational symmetry, and the gap function Eq. (7) becomes

$$\Delta_m(\mathbf{k}) = - \sum_{\mathbf{k}'} V_{mn}(\mathbf{k}, \mathbf{k}') \frac{\tanh(\beta E_{n\mathbf{k}'}/2)}{2E_{n\mathbf{k}'}} \Delta_n(\mathbf{k}') \quad (8)$$

where m, n are the band indices, $E_{n\mathbf{k}} = \sqrt{\Delta_n(\mathbf{k})^2 + \epsilon_n(\mathbf{k})^2}$, $\epsilon_n(\mathbf{k})$ is the single particle energy. The summation is taken only in the vicinity of Fermi pockets with an energy cut-off ω_D . The pairing potential $V_{m,n}(\mathbf{k}, \mathbf{k}')$ describes the coupling between gap function on various Fermi pockets, and with Eq. (4), we have

$$V_{mn}(\mathbf{k}, \mathbf{k}') = \sum_{\alpha} U_{m\alpha}(-\mathbf{k}) U_{m\alpha}(\mathbf{k}) U_{n\alpha}(\mathbf{k}') U_{n\alpha}(-\mathbf{k}') \times (g_0 + 4g_2 \cos q_x \cos q_y), \quad (9)$$

where m, n are band indices, α is orbital index, $U(\mathbf{k})$ is the transformation matrix between bands and orbitals.

In our two-orbital model, there are four Fermi pockets, two for hole bands at Γ and M points respectively and two for electron bands at X and Y points respectively, which makes it very difficult to solve Eq. (9) analytically. So in the following, we will ignore the size of the pockets and assume there are four point-like Fermi surfaces at

Γ , X , Y and M with finite density of states. And we also assume the summation in Eq. (8) are only over the four momentum $\Gamma = (0, 0)$, $Y = (\pi, 0)$, $X = (0, \pi)$, and $M = (\pi, \pi)$.

Then we consider the transformation matrix under this approximation. In the two-orbital model, the two orbitals, d_{xz} and d_{yz} , mixes strongly in the hole Fermi pockets. On the other hand, the two orbitals can be connected by a C_4 rotation. So in the case of point-like hole Fermi surface, it is obviously that the two orbitals contribute equally to the hole pockets, i.e. $U_{h,xz(yz)}[\Gamma(M)] = \frac{1}{\sqrt{2}}$, where h denotes the hole band and xz and yz denote the two orbitals. On the other hand, the two electron pockets are dominated by d_{xz} and d_{yz} orbital respectively. So under the small pocket approximation, we have $U_{e,xz}(Y) = U_{e,yz}(X) = 1$, and $U_{e,yz}(Y) = U_{e,xz}(X) = 0$. And the nonzero pairing potentials are $V_{hh}(\Gamma, \Gamma) = V_{hh}(\Gamma, M) = V_{hh}(M, M) = \frac{v_0}{2}$, $V_{ee}(X, X) = V_{ee}(Y, Y) = v_0$, and $V_{he}[\Gamma(M), X(Y)] = \frac{v_2}{2}$, where $v_0 = g_0 + 4g_2$ and $v_2 = g_0 - 4g_2$.

In the small pocket approximation, the gaps on the two electron pockets should be same because of the C_4 rotational invariance of the iron pnictide. Though the gaps on the hole pockets may be different, we still assume they are equal for simplicity. So with the above pairing potentials, we can solve the gap equation (8) and get the critical temperature

$$k_B T_c = 1.14 \omega_D e^{-1/N_h(0)\tilde{v}} \quad (10)$$

with $\tilde{v} = \frac{1}{2}[(1 + \lambda)(g_0 + 4g_2) + \sqrt{(1 + \lambda)^2(g_0 + 4g_2)^2 - 16\lambda g_0 g_2}]$, where $\lambda = N_e(0)/N_h(0)$, and $N_e(0)$ and $N_h(0)$ denote the density of state at the Fermi level of electron and hole pockets respectively.

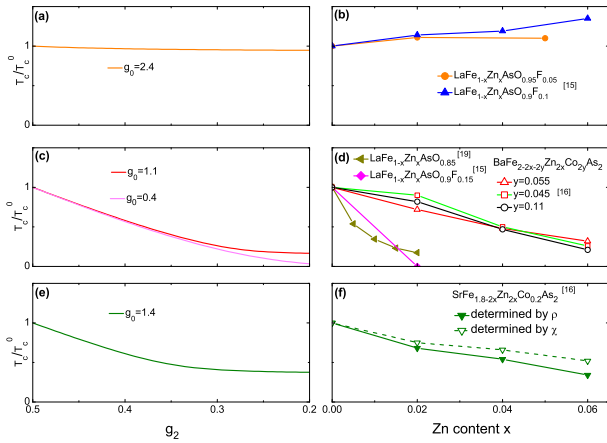


FIG. 3: (Color online) Left: The critical temperature T_c as a function of g_2 with strong, weak, and moderate on-site pairing coupling g_0 . Right: Zn-impurity effect on T_c in various Fe-based superconductors observed in experiments. The references of the data are listed.

Our calculation on the critical temperature for various impurity concentrations, depicted at the left panel of

Fig. 3, reveals that the different impurity-doping behaviors observed in FeSC [15, 16] may be characterized by the strength of the effective on-site pairing potential g_0 . There are three types of cases for the disorder effect. In the case of large g_0 , where the on-site pairing dominates, T_c is hardly suppressed by the Zn doping. In the case of weak g_0 , superconductivity is destroyed by the impurity. When g_0 is comparable with g_2 , as Zn impurity concentration increases, T_c is initially suppressed rapidly and then saturate. The experimental facts seem to support the above scenarios and the effect of Zn doping depends on the material and the charge carrier concentration. In $\text{LaFe}_{1-x}\text{Zn}_x\text{AsO}_{0.9}\text{F}_{0.1}$ (Ref. [14]), T_c are insensitive to the Zn-impurity, and may be explained due to large g_0 . In the over-doped $\text{LaFe}_{1-x}\text{Zn}_x\text{AsO}_{0.85}\text{F}_{0.15}$ (Ref. [15]) and $\text{LaFeAsO}_{0.85}$ (Ref. [19]), in $\text{BaFe}_{2(1-x-y)}\text{Zn}_{2x}\text{Co}_y\text{As}_2$ (Ref. [16]), and in $\text{LaFe}_{1-x-y}\text{Co}_y\text{Zn}_x\text{O}$ (Ref. [20]), T_c decreases rapidly with the Zn doping, and may belong to the category of weak g_0 . In $\text{SrFe}_{1.8-2x}\text{Zn}_{2x}\text{Co}_{0.2}\text{As}_2$ (Ref. [16]), T_c was found to decrease slowly and has the tendency to saturate although higher Zn-doping will be needed to confirm the speculation. These scenarios are summarized in Fig. 3, which shows the critical temperature vs g_2 at different g_0 compared with the experimental data of the three types of materials that behaves differently upon Zn doping.

The moderate value of g_2 case is most interesting, for it reflects the competition between the two SC pairings. To further explore this possibility, we have prepared $\text{SmFe}_{1-x}\text{Zn}_x\text{AsO}_{0.9}\text{F}_{0.1}$ system with $T_c = 50\text{K}$ and studied systematically the Zn-impurity effect to T_c experimentally. The results are summarized in Fig. 4. We have measured the change of the lattice constant due to Zn-doping and confirmed that Zn-atoms are indeed doped into the iron sites up to 6% of Zn doping, see Fig. 4(b) [21]. Beyond this doping, our data indicate that some Zn-impurity may not enter into Fe-lattice so the measurement of T_c may not correspond to the uniformly doped Zn-impurities. The main experimental result of T_c versus Zn concentration on this very high T_c material is plotted in Fig. 4(a). As we can see, as Zn is introduced, T_c reduces from 50K continuously down to 40K at 6% of Zn. The slow reduction in T_c may suggest that the superconductivity saturates at large Zn doping. It will be interesting to confirm this by doping high Zn concentration under high pressure, which remains a challenge in material preparation.

In addition to the critical temperature, another important feature during the transition from s_{\pm} to s_{++} is the change of low energy density of states (DOS). As shown in Fig. 5(a), the gap amplitude reduces accompanying with the increase of low energy DOS when the system approaches the transition point $n_{imp} \approx 0.04$ from clean limit. And if one further increases the impurity concentrations, the low energy DOS will be suppressed again due to the reopening of the gap. The non monotonic behavior of DOS with impurities concentration should be able to be observed by integrated photoemission spec-

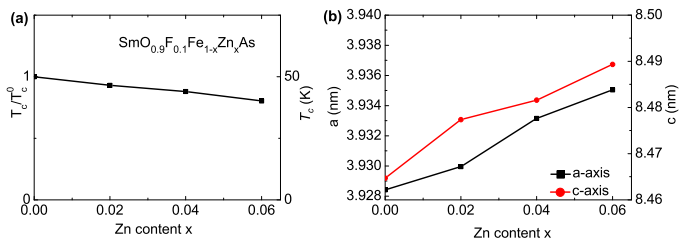


FIG. 4: (Color online) (a) T_c versus Zn-doping concentration for $\text{SmFe}_{1-x}\text{Zn}_x\text{AsO}_{0.9}\text{F}_{0.1}$. (b) Lattice constants a and c as functions of Zn-doping content in $\text{SmFe}_{1-x}\text{Zn}_x\text{AsO}_{0.9}\text{F}_{0.1}$.

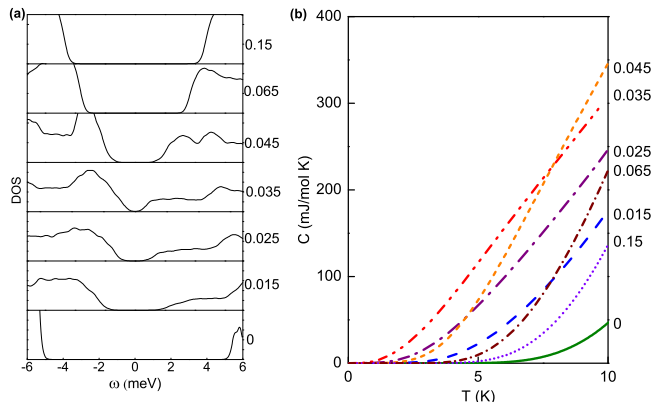


FIG. 5: (Color online) (a) DOS for various impurity concentrations. $n_{imp} = 0, 0.015, 0.025, 0.035, 0.045, 0.065$ and 0.15 from bottom to top. (b) The low temperature specific heat at various impurity concentrations.

troscopy.

The change of DOS with impurity concentration may also be observed by the experiments which can measure the low energy DOS, for example the specific heat. In the superconducting state, the electron specific heat can be calculated with

$$C(T) = \frac{\partial}{\partial T} \int_{-\infty}^{\infty} EN(E)f(E)dE, \quad (11)$$

where $N(E)$ is the DOS, and $f(E)$ is the Fermi distribution function. In the low temperature regime, the temperature dependence of the superconducting order parameter is very weak and can be neglected. So we use the zero-temperature DOS to calculate the specific heat with Eq. (11). In the calculation, we use $\Delta_{\text{coh}} = 0.18t_1 = 6\text{meV}$ as the energy scale, and the result is depicted in Fig. 5(b). We find that the electron specific heat below 10K is small in the clean limit, and shows a significant

increase with approaching the transition point by increasing impurity concentrations. When the system is stabilized in the s_{++} state, $C(T)$ drops to a low value again. And the absolute value shown in Fig. 5(b) is in the same order or even larger than the experimental measurement of 1111 material [22]. So it should be able to be observed in experiments.

We note the recent work of Efremov et al. [23], who applied T-matrix method to study the non-magnetic effect on FeSC. Our microscopic theory shares some similarities with their. In their phenomenological theory the impurity-doping behavior is found to be associated with the averaged pairing coupling strength. In our theory, the decisive role of on-site pairing on the impurity effect is identified.

V. SUMMARY

In summary, we have studied the disorder-induced pair-breaking effect on the Fe-based superconductors using a model that incorporates both the on-site and NNN pairings. We show that the Zn-impurity largely suppresses NNN pairing. Its effect to the superconductivity depends strongly on the on-site pairing coupling strength g_0 . The superconductivity can be robust, or evolves a transition from s_{\pm} to s_{++} , or is strongly suppressed in the presence of the disorder. Our theory qualitatively explains different reductions of T_c in various iron pnictide superconductors observed in the experiments on the Zn-impurity effect. We also predict the possible Zn-impurity doping induced transition from s_{\pm} to s_{++} pairing states in certain samples. Furthermore, we have systematically prepared Sm-1111 samples with $T_c = 50\text{K}$ under the Zn-doping and show that the reduction of T_c could be consistent with the scenario of a moderate on-site s-wave pairing. It will be highly interesting and important to prepare systematic controlled samples with higher Zn-doping to experimentally confirm or falsify the theory. The reduction of the gap in DOS during the transition from s_{\pm} to s_{++} can be observed by integrated photoemission spectroscopy or specific heat experiments. Finally we remark that the explicit pairing forms are unlikely to be universal in Fe-based superconductors, in contrast to the universal d -wave pairing in cuprates.

Acknowledgments

This work is partly supported by Hong Kong RGC grant and NSFC/RGC Joint Research Scheme (No. 10931160425 and No. N-HKU 726/09).

[1] H. Ding, P. Richard, K. Nakayama, K. Sugawara, T. Arakane, Y. Sekiba, A. Takayama, S. Souma, T. Sato,

T. Takahashi, et al., EPL (Europhysics Letters) **83**, 47001 (2008).

- [2] T. Sato, K. Nakayama, Y. Sekiba, P. Richard, Y.-M. Xu, S. Souma, T. Takahashi, G. F. Chen, J. L. Luo, N. L. Wang, et al., *Phys. Rev. Lett.* **103**, 047002 (2009).
- [3] C. Liu, G. D. Samolyuk, Y. Lee, N. Ni, T. Kondo, A. F. Santander-Syro, S. L. Bud'ko, J. L. McChesney, E. Rotenberg, T. Valla, et al., *Phys. Rev. Lett.* **101**, 177005 (2008).
- [4] I. I. Mazin, D. J. Singh, M. D. Johannes, and M. H. Du, *Phys. Rev. Lett.* **101**, 057003 (2008).
- [5] F. Wang, H. Zhai, Y. Ran, A. Vishwanath, and D.-H. Lee, *Phys. Rev. Lett.* **102**, 047005 (2009).
- [6] A. D. Christianson, E. A. Goremychkin, R. Osborn, S. Rosenkranz, M. D. Lumsden, C. D. Malliakas, I. S. Todorov, H. Claus, D. Y. Chung, M. G. Kanatzidis, et al., *Nature* **456**, 930 (2008).
- [7] C.-T. Chen, C. C. Tsuei, M. B. Ketchen, Z.-A. Ren, and Z. X. Zhao, *Nature Physics* **6**, 260 (2010).
- [8] M. L. Teague, G. K. Drayna, G. P. Lockhart, P. Cheng, B. Shen, H.-H. Wen, and N.-C. Yeh, *Phys. Rev. Lett.* **106**, 087004 (2011).
- [9] T. Hanaguri, S. Niitaka, K. Kuroki, and H. Takagi, *Science* **328**, 474 (2010).
- [10] P. J. Hirschfeld, M. M. Korshunov, and I. I. Mazin, *Reports on Progress in Physics* **74**, 124508 (2011), 1106.3712.
- [11] C. Liu, T. Kondo, R. M. Fernandes, A. D. Palczewski, E. D. Mun, N. Ni, A. N. Thaler, A. Bostwick, E. Rotenberg, J. Schmalian, et al., *Nature Physics* **6**, 419 (2010), 0910.1799.
- [12] G. Levy, R. Sutarto, D. Chevrier, T. Regier, R. Blyth, J. Geck, S. Wurmehl, L. Harnagea, H. Wadati, T. Mizokawa, et al., *Phys. Rev. Lett.* **109**, 077001 (2012).
- [13] T. Berlijn, C.-H. Lin, W. Garber, and W. Ku, *Phys. Rev. Lett.* **108**, 207003 (2012).
- [14] Y. Li, X. Lin, Q. Tao, C. Wang, T. Zhou, L. Li, Q. Wang, M. He, G. Cao, and Z. Xu, *New Journal of Physics* **11**, 053008 (2009).
- [15] Y. Li, J. Tong, Q. Tao, C. Feng, G. Cao, W. Chen, F. chun Zhang, and Z. an Xu, *New Journal of Physics* **12**, 083008 (2010).
- [16] J. Li, Y. Guo, S. Zhang, Y. Tsujimoto, X. Wang, C. Sathish, S. Yu, K. Yamaura, and E. Takayama-Muromachi, *Solid State Communications* **152**, 671 (2012), ISSN 0038-1098.
- [17] S. Raghu, X.-L. Qi, C.-X. Liu, D. J. Scalapino, and S.-C. Zhang, *Physical Review B* **77**, 220503 (2008).
- [18] The impurity also slightly affects the on-site pairing gap.
- [19] Y. F. Guo, Y. G. Shi, S. Yu, A. A. Belik, Y. Matsushita, M. Tanaka, Y. Katsuya, K. Kobayashi, I. Nowik, I. Felner, et al., *Phys. Rev. B* **82**, 054506 (2010).
- [20] Li, Yuke *et al*, unpublished.
- [21] As seen in Fig. 4(b), the lattice constant a decreases slightly with the Zn doping, while c increases obviously. As a result, the cell volume of LaFeZnOF increase monotonously with increasing Zn content. Note that the lattice constant of LaOZnAs is larger than that of LaOFeAs [see *Inorg. Chem.* **37**, 386 (1998)]. The energy-dispersive x-ray spectrometry (EDX) analysis measurement shows that the actual Zn content in these samples is very consistent with the nominal composition, which suggests that Zn impurities should be successfully doped into the lattice.
- [22] G. Mu, H. Luo, Z. Wang, L. Shan, C. Ren, and H.-H. Wen, *Phys. Rev. B* **79**, 174501 (2009).
- [23] D. Efremov, M. Korshunov, O. Dolgov, A. Golubov, and P. Hirschfeld (2011), arXiv:1104.3840.